

TECHNICAL REPORTS: METHODS

10.1002/2015WR017693

Key Points:

- The Advection-Aridity model is used with an enhanced wind function
- An aridity function is introduced into the Complementary Relationship of evaporation
- Model explains 90% of the spatial variation in HUC6-averaged mean annual runoff

Correspondence to:

J. Szilagyi,
jszilagy1@unl.edu

Citation:

Szilagy, J. (2015), Complementary-relationship-based 30 year normals (1981–2010) of monthly latent heat fluxes across the contiguous United States, *Water Resour. Res.*, 51, 9367–9377, doi:10.1002/2015WR017693.

Received 12 JUN 2015

Accepted 10 NOV 2015

Accepted article online 12 NOV 2015

Published online 22 NOV 2015

Complementary-relationship-based 30 year normals (1981–2010) of monthly latent heat fluxes across the contiguous United States

Jozsef Szilagyi^{1,2}

¹Department of Hydraulic and Water Resources Engineering, Budapest University of Technology and Economics, Budapest, Hungary, ²School of Natural Resources, University of Nebraska-Lincoln, Lincoln, Nebraska, USA

Abstract Thirty year normal (1981–2010) monthly latent heat fluxes (ET) over the conterminous United States were estimated by a modified Advection-Aridity model from North American Regional Reanalysis (NARR) radiation and wind as well as Parameter-Elevation Regressions on Independent Slopes Model (PRISM) air and dew-point temperature data. Mean annual ET values were calibrated with PRISM precipitation (P) and validated against United States Geological Survey runoff (Q) data. At the six-digit Hydrologic Unit Code level (sample size of 334) the estimated 30 year normal runoff ($P - ET$) had a bias of 18 mm yr^{-1} , a root-mean-square error of 96 mm yr^{-1} , and a linear correlation coefficient value of 0.95, making the estimates on par with the latest Land Surface Model results but without the need for soil and vegetation information or any soil moisture budgeting.

1. Introduction

With a changing climate and an expected intensification of the global hydrologic cycle, accurate determination of the latent heat fluxes (ET) between the land surface and the ambient atmosphere over extended time intervals and/or extensive areas is crucial for, e.g., hydroclimatological predictions and simulations, as well as long-term and/or large-scale water management operations including drought monitoring and flood alleviation. While remote-sensing based ET estimation methods are evolving fast (for a review, see Wang and Dickinson [2012]), reanalysis-based methods [Chen et al., 1997; Koster and Suarez, 1996; Liang et al., 1994; Mesinger et al., 2006] are also important because of their longer temporal coverage, their insensitivity to cloud cover, and because they may form part of remote-sensing based ET estimation techniques [Szilagyi et al., 2011; Wu et al., 2014]. Reanalysis data are considered as the best representation of reality for spatially distributed, long-term applications, since they combine measurements with modeling results by taking into account the errors in both. The North American Regional Reanalysis (NARR) data [Mesinger et al., 2006] are an improvement on continental-scale reanalyses due to its finer resolution (i.e., 32 km), its state-of-the-art Land Surface Model (LSM) component, and the assimilation of observed precipitation for the North American continent and adjacent oceans over the past 35 years [Sheffield et al., 2012]. The LSMs provide sensible (H) and latent heat fluxes typically employing variations of the Penman-Monteith equation [Monteith, 1965] for the latter, requiring soil and vegetation information to perform soil moisture budgeting. Considering the typically large heterogeneity in soil type, thickness, layering, vegetation-cover, and rooting depth, the ensuing ET fluxes may contain a relatively high degree of uncertainty, resulting in noticeable differences in ET values among LSM versions [Sheffield et al., 2012], giving rise to the need for an alternative formulation of the ET fluxes not requiring soil, land surface or vegetation information.

2. Application of the Complementary Relationship

The complementary relationship (CR) of regional evaporation [Bouchet, 1963] scales the wet-environment ET rate, ET_w , to actual ET rate by comparing the spatially averaged latent heat fluxes of wet surfaces differing only in size: that of a small wet patch (e.g., a wet meadow) with a horizontal extent of $\sim 100 \text{ m}$ to one with an extent in excess of $\sim 1 \text{ km}$, the scale ET_w in fact is valid at. The more the small wet patch ET rate, ET_p ,

differs from ET_w due to horizontal energy advection, the drier the environment has become, therefore the lower actual ET is. ET_w is traditionally given [Brutsaert and Stricker, 1979] by the Priestley-Taylor equation [Priestley and Taylor, 1972] as:

$$ET_w = \alpha \frac{\Delta(T_w)}{\Delta(T_w) + \gamma} R_n. \quad (1)$$

Here R_n is the available energy (i.e., net radiation) at the wet surface, specified in water depth per unit time (i.e., mm d^{-1}), Δ is the slope of the saturation vapor pressure curve at the wet-environment air temperature (T_w), and $\gamma [= c_p p / (0.622L)]$ is the psychrometric constant, where c_p is the specific heat of air at constant pressure (p) and L is latent heat of vaporization for water. The coefficient $\alpha (>1)$ is generally accepted to express the evaporation-enhancing effect of large-scale entrainment of drier free-tropospheric air resulting from the growing daytime convective boundary layer [Brutsaert, 1982; de Bruin, 1983; Culf, 1994; Lhomme, 1997; Heerwaarden et al., 2009; Rigby et al., 2015].

The latent heat flux (in mm d^{-1}) of the small wet patch is defined by the Penman [1948] equation:

$$ET_p = \frac{\Delta(T_a)}{\Delta(T_a) + \gamma} R_n + \frac{\gamma}{\Delta(T_a) + \gamma} f_u (e^* - e_a), \quad (2)$$

where T_a is the air temperature over the drying land surface, e_a is the actual vapor pressure in hPa, e^* is the saturation vapor pressure at T_a , f_u is the (so-called Rome) wind function, traditionally expressed [Brutsaert, 1982] as:

$$f_u = 0.26(1 + 0.54u_2), \quad (3)$$

where u_2 is the wind speed (m s^{-1}) at 2 m above the ground.

The CR obtains actual ET as:

$$ET = ET_w - (ET_p - ET_w) / b, \quad (4)$$

where b^{-1} is a proportionality coefficient [Kahler and Brutsaert, 2006; Szilagyi, 2007]. When the time-rate of change in ET_p is similar to the one in ET (but with an opposite sign) during wetting/drying of the environment, b^{-1} becomes a constant unity, and the CR symmetric [Brutsaert and Stricker, 1979], otherwise b^{-1} depends on the aridity of the environment [Szilagyi, 2007]. The CR with Δ evaluated at T_a in (1) and (2) is called the Advection-Aridity (AA) model [Brutsaert and Stricker, 1979]. Morton's [1983] evaporation model also employs a symmetric CR but without wind data. Rather, it introduces an atmospheric stability function, defines ET_p so that it yields values very close to class-A pan evaporation rates, and linearly transforms (1) written for an open water surface. McMahon et al. [2013a] in a comprehensive study found the CR-based methods to be the most reliable practical ET estimation techniques available today, requiring only standard meteorological variables.

Notice that the air temperatures are different in (1) and (2) when the environment is not wet, which is typical. Therefore, it is necessary to estimate T_w from drying conditions. Szilagyi and Jozsa [2008] recommended an implicit formula based on the Bowen ratio (B_o) written for the small wet patch with daily sums of the fluxes as:

$$B_o = \frac{H}{ET_p} \approx \frac{R_n - ET_p}{ET_p} \approx \gamma \frac{T_{ws} - T_a}{e^*(T_{ws}) - e(T_a)} \quad (5)$$

making use of the assumptions that R_n , T_a , and e_a over the drying and wet surfaces are about the same due to the small extent of the latter. T_{ws} is the estimated air temperature at the wet surface, which has recently been shown to be constant [Szilagyi and Schepers, 2014] in space and time under constant (temporally and spatially) R_n and wind conditions during drying of the environment around the wet patch. Since the equilibrium air temperature profile over wet surfaces has a mild gradient with height above the ground [Szilagyi and Jozsa, 2009], the T_{ws} value estimated from (5) can be taken for T_w as long as $T_{ws} < T_a$, otherwise T_w can be replaced by T_a [Huntington et al., 2011; McMahon et al., 2013a,b; Szilagyi, 2014a].

Table 1. List of Functions (After Fenicia et al. [2011]) Applied for b^{-1}

Functional Form of $b^{-1} = f(RH p, q)$	Name	Parameter (p, q) Range
$RH = \text{const.}$	Constant	$p = 0.7-1$
RH	Identity function	
$(RH)^p$	Power function	$p = 0.13-1.5$
$1 - (1 - RH)^p$	Reflected power function	$p = 1-3$
$(1 + p) RH / (RH + p)$	Monod-type kinetics	$p = 0.4-0.6$
$(1 + e^{-p(1-q)})(e^{-pRH} - 1) / (1 + e^{-p(RH-q)})(e^{-p} - 1)$	Modified logistic curve	$p = 1-20, q = 0.1-1$
$[E_p(\text{Rome } f_u) / E_p(\text{pan } f_u)]^p$	Pan coefficient	$p = 0.5-2$
$p \gamma / \Delta(T_a)$	Szilagyi [2007]	$p = 1$

Szilagyi and Jozsa [2008] demonstrated that by prescribing a suitable (pan) wind function:

$$f_u = 0.49(1 + 0.35u_2), \tag{6}$$

(2) can be applied for estimating monthly class-A pan evaporation rates in moderately dry regions. As was shown by Kahler and Brutsaert [2006], class-A pan evaporation is more sensitive to changes (i.e., drying) in the surrounding environment than a small wet patch, therefore better poised for detecting small changes in actual ET , provided the proportionality/aridity function, b^{-1} , is well defined. While the CR, (4), with the original Penman equation (i.e., (2) with the Rome wind function, (3)) tends to be symmetric ($b^{-1} \approx 1$) [Brutsaert and Stricker, 1979; Hobbins et al., 2001a,b; Ramirez et al., 2005; Szilagyi et al., 2009; Huntington et al., 2011; Szilagyi, 2014a], it becomes highly asymmetrical with class-A pan evaporation rates [Ramirez et al., 2005; Kahler and Brutsaert, 2006; Szilagyi and Jozsa, 2008].

In this study an asymmetric CR, i.e., (2) with (6), is applied to estimate the 30 year normals (1981–2010) of monthly ET rates across the contiguous United States, making use of the North American Regional Reanalysis (NARR) radiation and 10 m wind (u_{10}) as well as Parameter-Elevation Regressions on Independent Slopes Model (PRISM) precipitation (P), air and dew-point temperature (T_d) data [Daly et al., 1994] at a spatial resolution of 4 km. The monthly mean PRISM T_d values are only available as 30 year normals therefore the ensuing ET estimation could not be performed on a continuous month-by-month basis, but rather as 30 year normals using similar averages of the input variables. Monthly u_{10} values were transformed to u_2 via $u_2 = u_{10} (2/10)^{1/7}$ [Brutsaert, 1982].

3. Calibration of the CR

Hobbins et al. [2001b] demonstrated that the CR-based AA model [Brutsaert and Stricker, 1979] improves with local calibration of its wind function. Similar local calibration of Morton’s CR model [1983] is not easily viable because of its several globally optimized empirical parameters (e.g., the air stability function). While locally calibrating the wind function may lead to better AA-model performance, a more general approach that does not need such calibration is preferable, as data for local calibration may often be lacking. Szilagyi et al. [2009] demonstrated that AA-model performance improves, especially in hot and dry climates, by simply accounting for the changes in air temperature between (1) and (2). Therefore ET rates at the 4 km PRISM resolution are estimated here by substituting the T_{ws} estimates (as a proxy of T_w) of (5) into (1) and employing (2) and (6) in (4) through the calibration of the proportionality coefficient, b^{-1} , as a function of aridity [Szilagyi, 2007].

While aridity can be defined in several ways, the relative humidity, $RH = e^*(T_d)/e^*(T_a)$, as a proxy measure of aridity is used here in order to avoid introducing additional input variables to the model. Table 1 lists the types of the aridity functions considered during calibration. They all increase with RH (except the first one, while the last one in its tendencies, since with wetting of the environment RH increases while T_a tends to decrease) in accordance with the CR and yield values between zero and unity. The objective function of calibration consisted of minimizing the following two quantities for the 30 year normal annual values: (a) the number of cells with $ET > P$, and; (b) the number of cells with $ET = 0$. Notice that (a) no other information (e.g., runoff for water balancing) was used for the calibration; (b) the two conditions somewhat counteract each other (the first depresses, while the second inflates ET), pressing the modeled ET rates into a realistic interval in most parts of the study area. Note also that calibration does not prevent the resulting values to exceed precipitation rates as indeed $ET > P$ occurs on a long-term basis even at a regional scale [Szilagyi, 2013, 2014b].

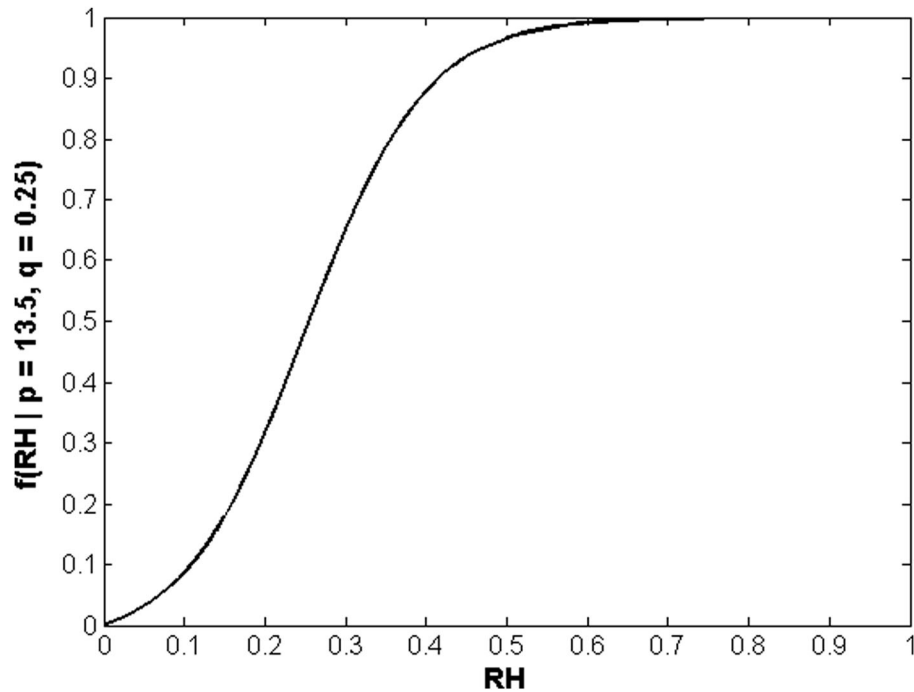


Figure 1. The optimized logistic curve-type aridity function, b^{-1} , of Table 1.

During the trial-and-error calibration the value of α in (1) was also changed systematically between 1.1 and 1.3 for each parameter value of Table 1. Eventually, the modified logistic curve (Figure 1) provided the best *ET* estimates (shown below) with $p = 13.5$, $q = 0.25$, and $\alpha = 1.23$. It shows that in humid to mildly humid conditions ($RH > 0.5$) the CR is near-symmetric, a property that progressively breaks down with increasing aridity. Figure 2 displays the sensitivity of several model performances to changes in calibrated parameter values, proving the value of α to be the most critical.

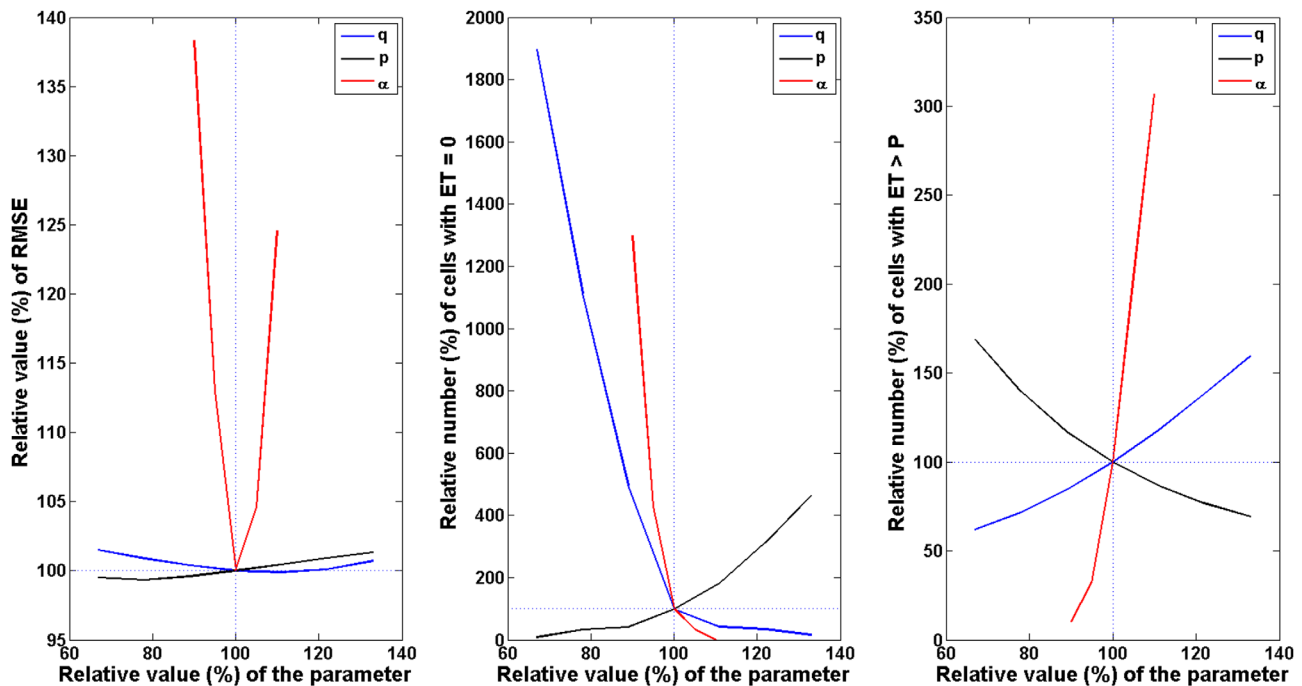


Figure 2. Sensitivity of model performance to changes in calibrated parameter values. RMSE is the root-mean-square error of the 30 year normal annual *ET* rates averaged over the 334 United States Geological Survey (USGS) six-digit (HUC6) watersheds that cover the conterminous US.

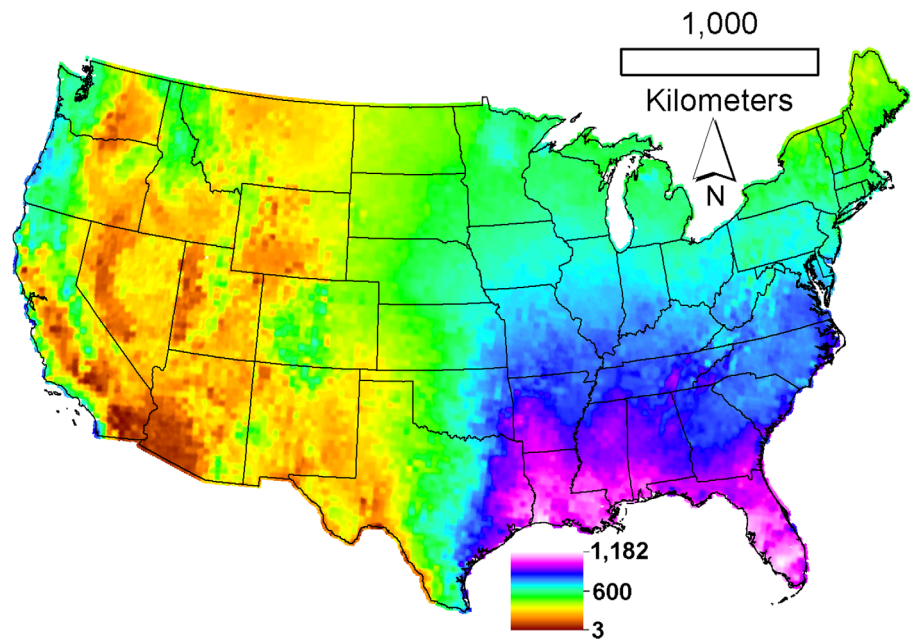


Figure 3. Spatial distribution of the 30 year normal (1981–2010) annual ET (mm yr^{-1}) estimates. $\langle ET \rangle = 522 \pm 228 \text{ mm yr}^{-1}$.

4. Results and Discussion

Estimated long-term mean annual ET (Figure 3) is zero in only 59 PRISM grid-points (in California and southwestern Arizona) from a total of 481,631 grid point values over the contiguous US, with a sample mean, $\langle ET \rangle = 522 \pm 228 \text{ mm yr}^{-1}$. Estimated ET exceeds precipitation in 55,519 ($\sim 12\%$ of the total) grid points (Figure

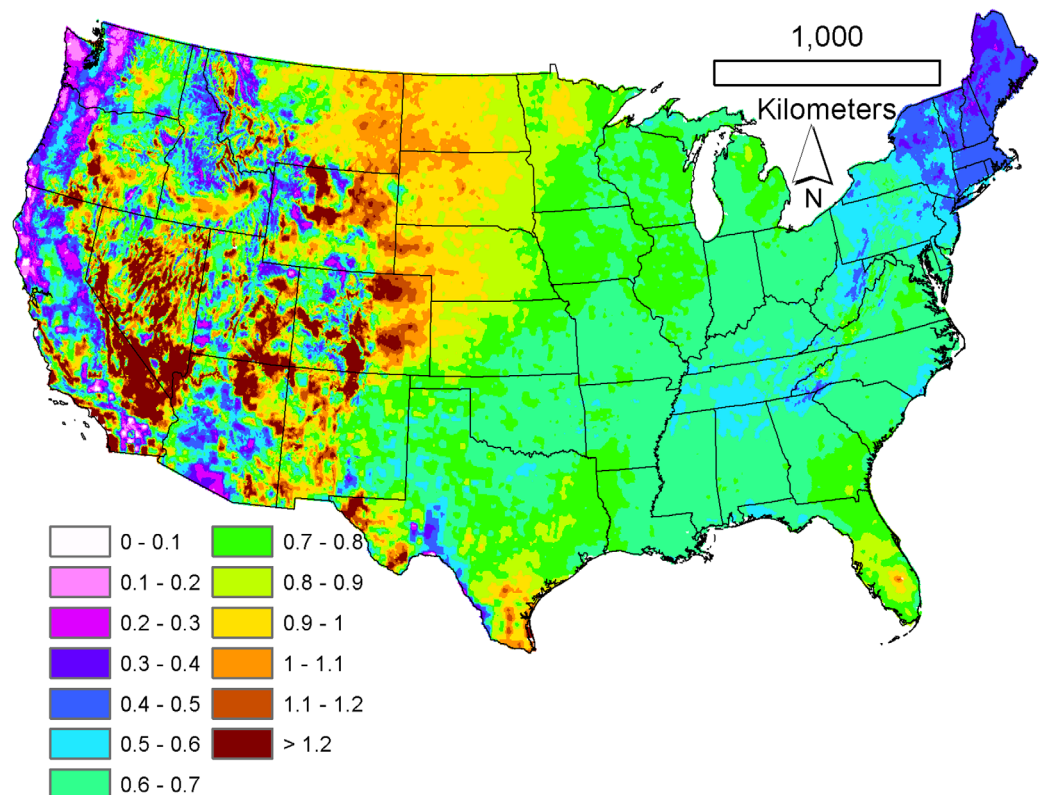


Figure 4. Spatial distribution of the ratio of 30 year normal annual ET and PRISM precipitation.

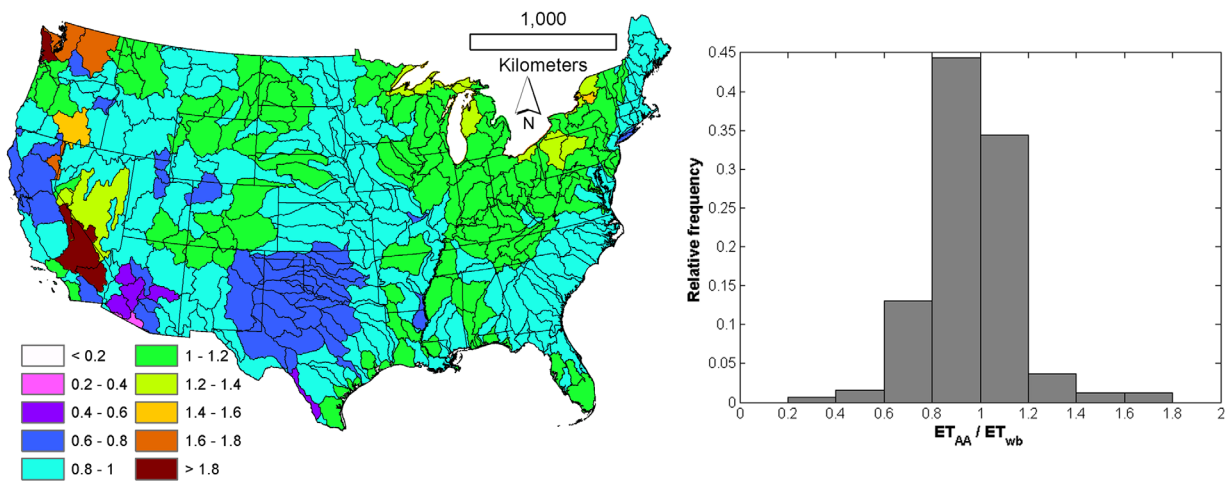


Figure 5. Distribution of the ratios of HUC6-averaged CR- (ET_{AA}) and simplified water-balance-derived (ET_{wb}) 30 year normal annual ET and their histogram ($n = 334$).

4), but rarely by more than 20% of the PRISM precipitation value, typically in valleys and basins of the western states. The area-weighted sample ($n = 334$) mean of the simplified water-balance approach, i.e., the difference between the PRISM P values averaged over the HUC6 watersheds and the corresponding runoff, Q (source: waterwatch.usgs.gov), yields $537 \pm 228 \text{ mm yr}^{-1}$, a departure of less than 3% from the CR-based value.

Note that the watershed drainage area values contain varying portions of the Great Lakes surface areas therefore the HUC6 area-weighted 30 year normal of annual PRISM P becomes 786 instead of the original spatial average of $791 \pm 448 \text{ mm yr}^{-1}$ due to the absence of P values over the lakes.

Figure 5 displays the spatial distribution of the CR- and water-balance-derived mean annual ET ratios and their histogram. The CR-derived and HUC6-averaged ET is within 20% of the water-balance obtained value over 80% of the catchments.

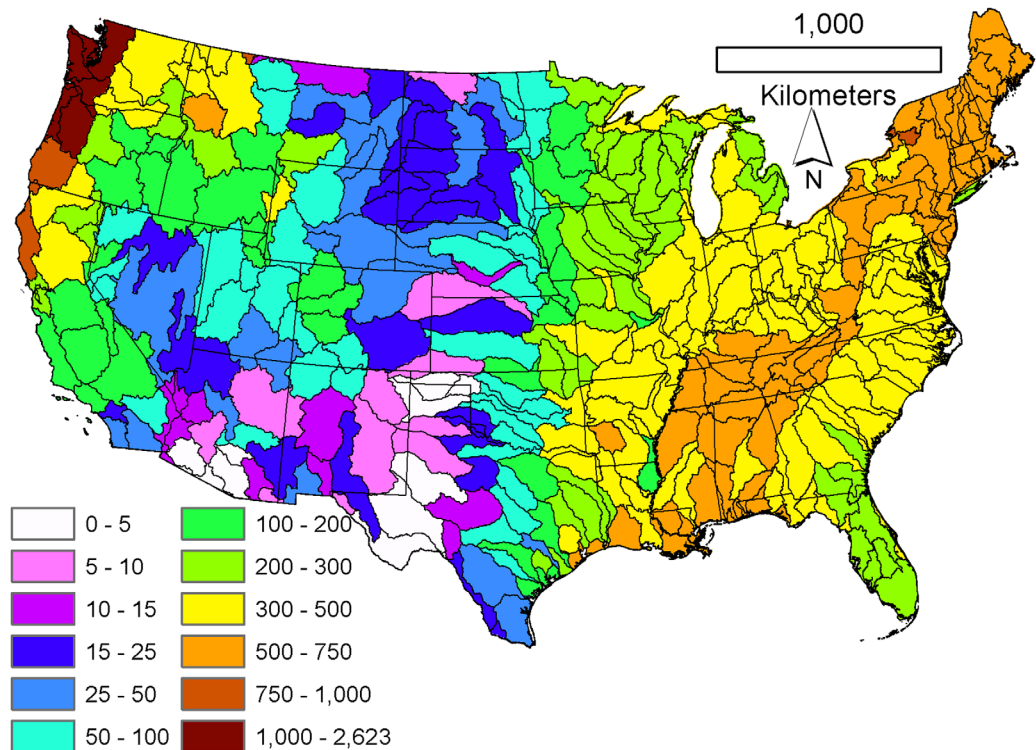


Figure 6. Spatial distribution of the HUC6-averaged 30 year normal annual USGS runoff (Q) rates (mm yr^{-1}). $\langle Q \rangle = 249 \pm 270 \text{ mm yr}^{-1}$.

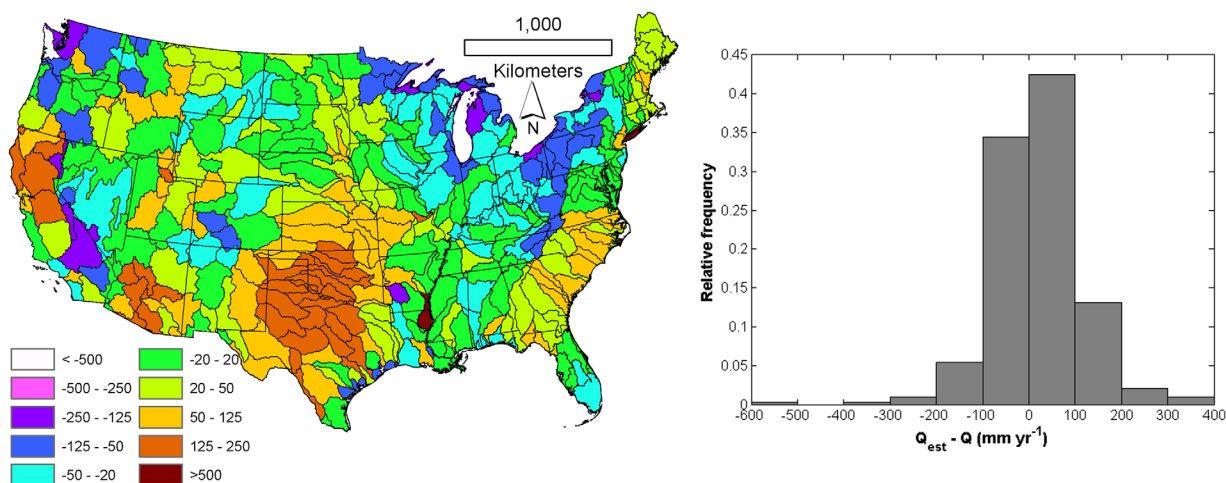


Figure 7. Spatial distribution of the difference in the HUC6-averaged CR-derived ($Q_{est} = P - ET_{AA}$) and USGS-measured (Q) 30 year normal annual runoff rates (mm yr^{-1}) and their histogram ($n = 334$).

The CR underestimates water-balance ET the most significantly in south-western Arizona, and overestimates it in the Mojave Desert of California and in Washington State, locations with the two extremes (i.e., driest and wettest) of precipitation within the conterminous US (Figure 4). Even within the driest region, runoff varies significantly, from less than 5 mm yr^{-1} (south-western Arizona) to over 100 mm yr^{-1} in the Mojave Desert (Figure 6) while corresponding catchment-averaged precipitation (not displayed) remains between 140 and 170 mm yr^{-1} .

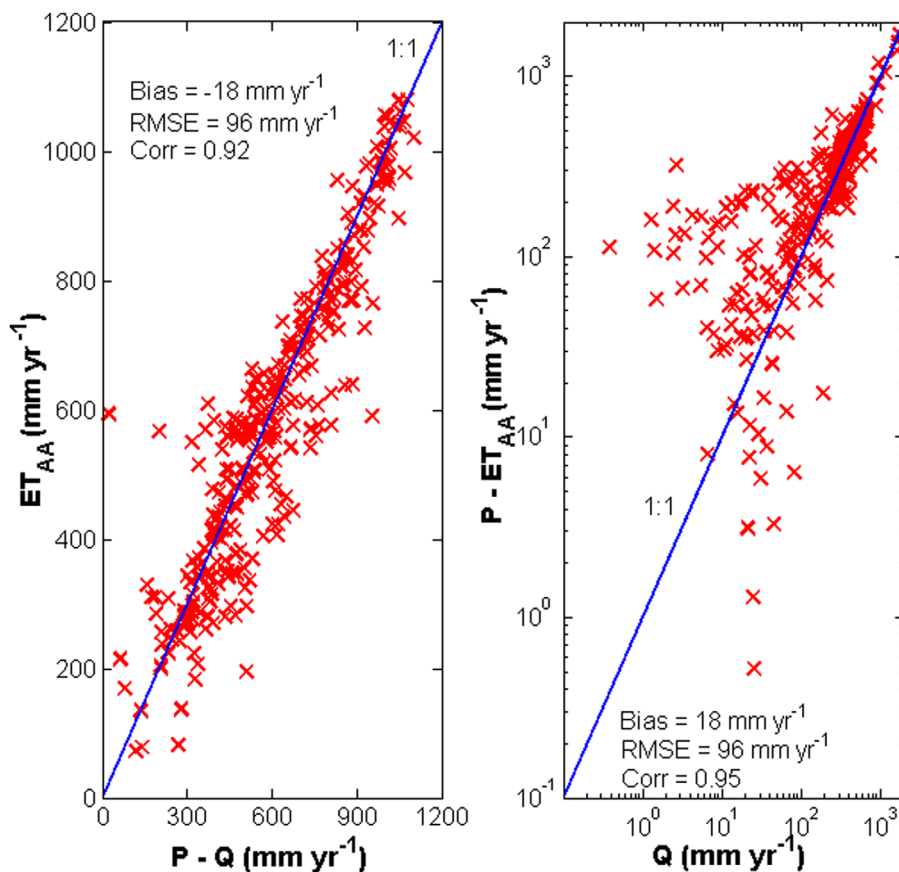


Figure 8. Regression plots of HUC6-averaged a) CR-derived and simplified water-balance derived 30 year normal annual ET ; (b) CR-derived ($P - ET_{AA}$) and measured (Q) runoff values ($n = 334$).

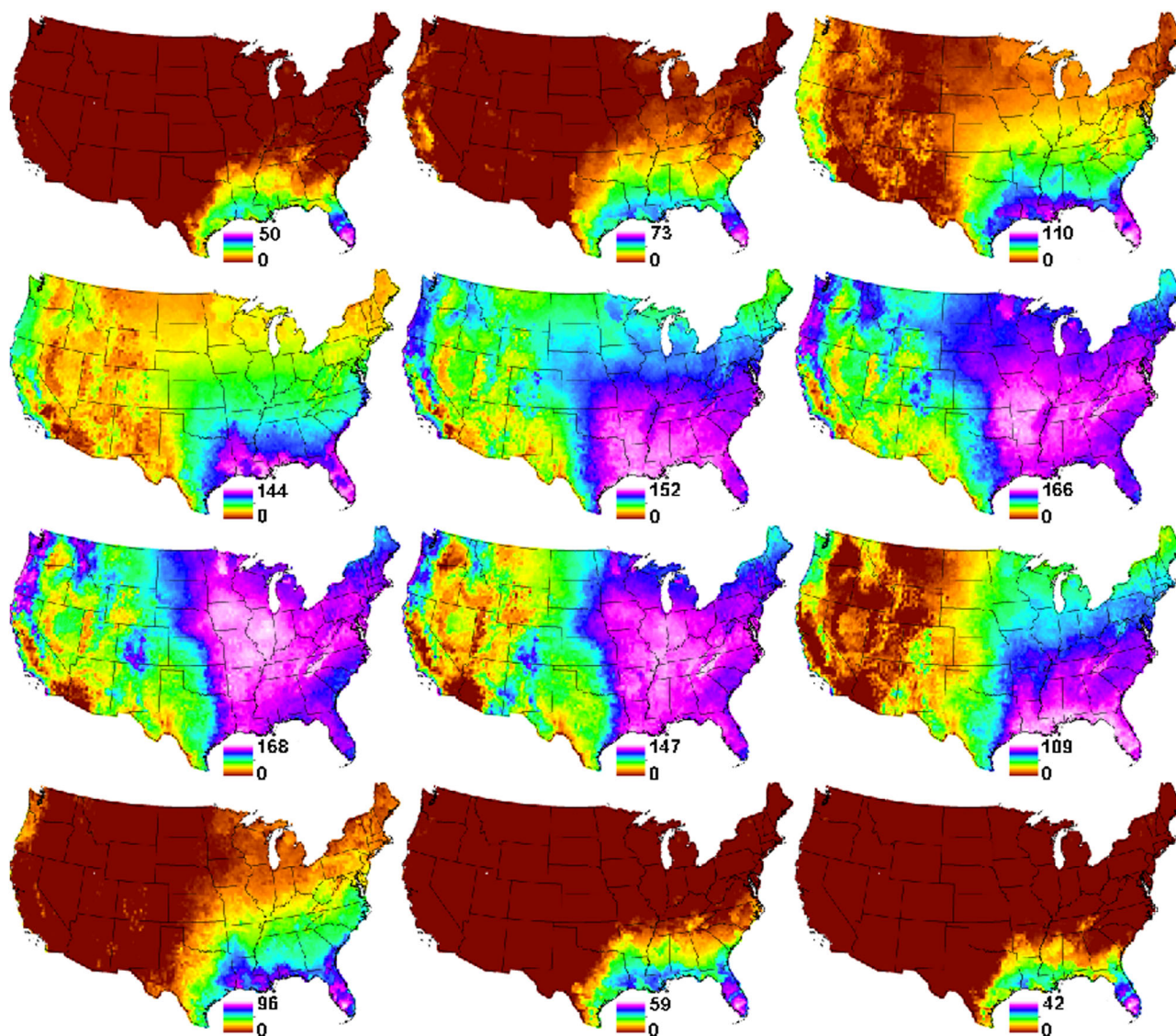


Figure 9. Spatial distribution of the AA-estimated 30 year normal monthly ET rates (mm mo^{-1}). The months are row-continuous (i.e., first row: January–February–March).

The situation is even more interesting in the West Texas and Oklahoma panhandle watersheds, displaying less than 5 mm yr^{-1} runoff while enjoying $344\text{--}572 \text{ mm}$ of precipitation annually, resulting in runoff ratios of only a few percent. With this significant spatial variability in runoff, the AA-derived ET rates yield runoff rates that are within 100 mm of the measured value in more than 75% of the catchments (Figure 7) or within 50–200% of measured Q in 75% of the watersheds. From the 334 value pairs of Figure 8, water-balance ET and the corresponding runoff rate are under/overestimated by only 18 mm yr^{-1} on average, with a root-mean-square error ($RMSE$) of 96 mm yr^{-1} and a linear correlation coefficient ($Corr$) value of 0.92 and 0.95, respectively. The latter means that the present AA-model can explain about 90% of the variation found in the HUC6 30 year normal annual runoff rates, indicative of a robust model. These performance indicators are similar (or better than) to the ones reported by recent LSMs [Sheffield *et al.*, 2012].

While at a long-term annual basis the estimated ET rates can be verified with simplified water-balance data, the monthly values cannot (Figure 9). Still some interesting patterns emerge from the estimated 30 year normal monthly ET rates. Some examples: (a) US-wide ET is not symmetrical over the year. ET is larger in general in the first part of the year, reaching a peak in June/July (106 and 105 mm , respectively). (b) In February, the largest ET contributor in the West is the Central Valley of California, due to mild

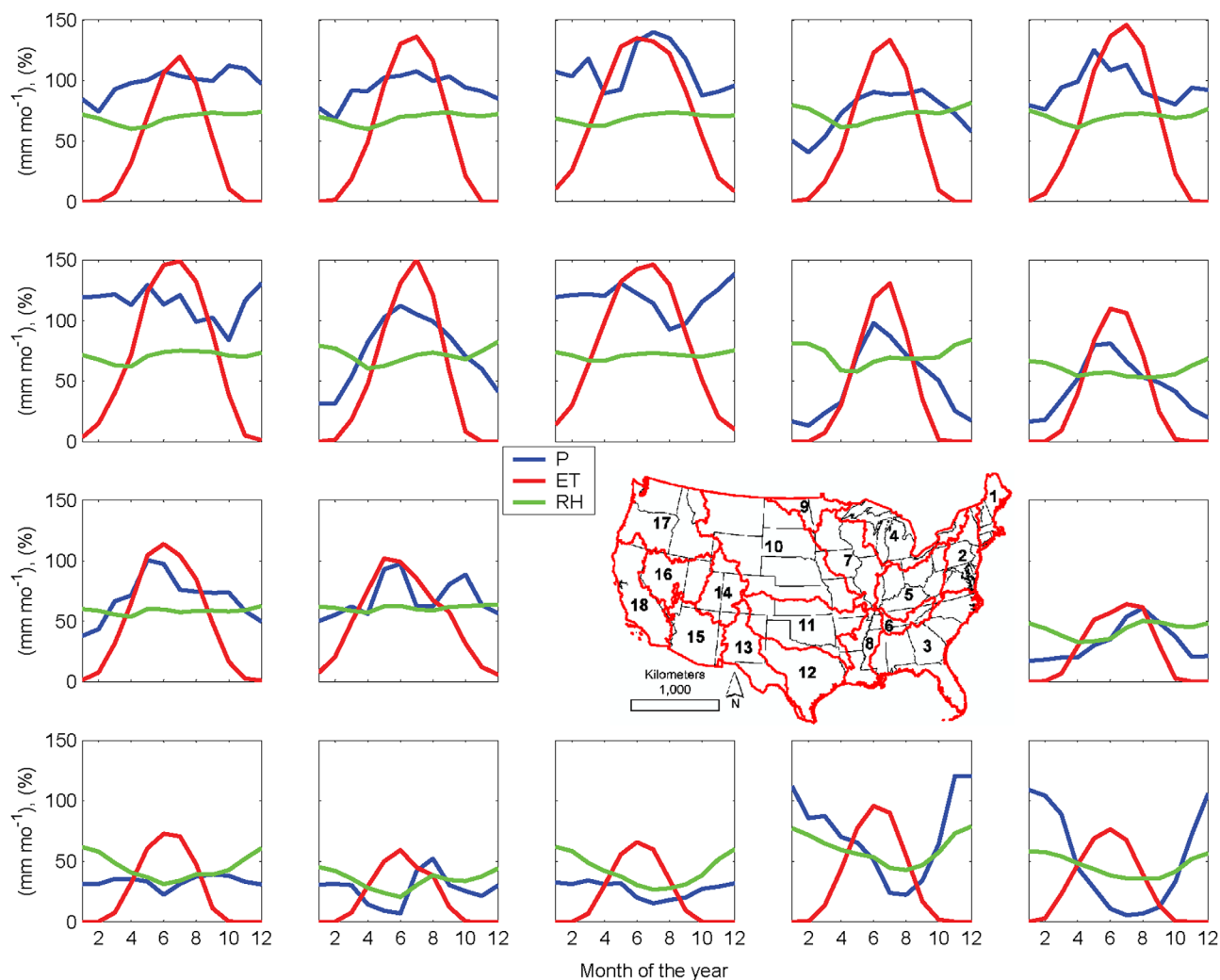


Figure 10. Thirty year normals of the monthly ET , P , and RH values by two-digit HUC regions (row continuous).

temperatures and winter rains. (c) Over the Rockies in general, ET rates in March shoot up first in the mountains, probably due to enhanced precipitation year round. (d) Dry out in the West starts first in Southern California and Arizona in July and spreads northward. (e) The large wetland area in Northern Minnesota stands out of its surroundings with its elevated ET rates during the entire warm season (April–September). (f) From April to August, ET rates are not the highest in Florida, but in different other Southern states, varying by month. (g) From June to August, ET is the largest in Nebraska among the prairie states along the 100th meridian (the north-south borderline between Texas and Oklahoma), even though annual precipitation is not. Nebraska, however, is the most intensively irrigated state (by irrigated area) within the US [United States Department of Agriculture (USDA), 2014] with peak water use in June and July. The effect of irrigation is reported [Kustu *et al.*, 2011] to be felt as far as Ohio in the form of increased summer rain and streamflow.

Figure 10 displays the monthly 30 year normals of the P , ET and RH values for the 18 two-digit HUC regions (HUC2) across the conterminous US. ET follows a more regular curve over the year than precipitation and peaks either in June or July, with the only May peak occurring in HUC2 #12, covering the bulk of Texas. The ET peaks are typically larger than similar peaks in precipitation, except in HUC2 #3, 17, and 18. The largest phase shifts between P and ET are found in HUC2 #16–18 as the result of a Mediterranean-type climate. The driest regions, with the smallest overall P , ET , and RH values are found in HUC2 #15 and 16 over Arizona, western Utah, and Nevada, Arizona being the only state where the monthly RH normals never reach 50%.

5. Summary and Conclusions

The Complementary Relationship of evaporation, after more than half a century of its inception [Bouchet, 1963] and undeniable success [McMahon et al., 2013a,b] is still a widely overlooked and underemployed tool in hydrology, climatology, and in the general area of water resources management. To this day, it is the only method that considers the complex interplay between soil moisture, vegetation, evapotranspiration, and water vapor content of the air and derives the corresponding ET rate from standard meteorological measurements only, without the need of information on the interacting land-soil-vegetation components. It is believed by this author that its application in LSMs as a calibration/verification tool would greatly improve the predictive capacity of such models.

Here a modified version of the CR-based AA model [Brutsaert and Stricker, 1979; Szilagyi et al., 2009] was employed for mapping 30 year (1981–2010) normals of monthly and annual latent heat fluxes across the contiguous US. Modifications included the choice of the wind function to increase the sensitivity of the CR, and the formulation as well as calibration of an aridity-based (relative humidity used as a proxy measure of aridity) proportionality function of the CR. Calibration was performed employing only precipitation measurements while validation was achieved by the help of watershed-averaged measured runoff.

The resulting long-term mean annual ET estimates explain 90% of the spatial variation found in measured HUC6 watershed-averaged runoff, with a bias of 18 mm yr^{-1} and $RMSE$ of 96 mm yr^{-1} , making the estimates on par with latest LSM results [Sheffield et al., 2012].

Future research could explore how different input data sets affect the shape of the aridity function, as it is not expected to be universal, but rather dependent on the data source employed.

Acknowledgments

This work has been supported by the Agricultural Research Division of the University of Nebraska-Lincoln. All data used in this study are publicly available from the following sites: waterwatch.usgs.gov (runoff data), www.prism.oregonstate.edu (PRISM data), www.esrl.noaa.gov/psd/data/gridded/data.narr.html (NARR data). Modeled spatially distributed data of this study are available from the author upon request. The author is thankful for the three anonymous reviewers for their valuable comments that lead to a much improved manuscript.

References

- Bouchet, R. J. (1963), Evapotranspiration réelle, evapotranspiration potentielle, et production agricole, *Ann. Agron.*, *14*, 543–824.
- Brutsaert, W. (1982), *Evaporation into the Atmosphere: Theory, History and Applications*, D. Reidel, Dordrecht, Netherlands.
- Brutsaert, W., and H. Stricker (1979), An advection-aridity approach to estimate actual regional evapotranspiration, *Water Resour. Res.*, *15*(2), 443–449.
- Chen, F., Z. Janjic, and K. Mitchell (1997), Impact of atmospheric surface-layer parameterizations in the new land-surface scheme of the NCEP mesoscale Eta model, *Boundary Layer Meteorol.*, *85*, 39–421.
- Culf, A. D. (1994), Equilibrium evaporation beneath a growing convective boundary layer, *Boundary Layer Meteorol.*, *70*, 37–49.
- Daly, C., R. P. Neilson, and D. L. Phillips (1994), A statistical topographic model for mapping climatological precipitation over mountainous terrain, *J. Appl. Meteorol.*, *33*, 140–158.
- de Bruin, H. A. R. (1983), A model for the Priestley-Taylor parameter α , *J. Clim. Appl. Meteorol.*, *22*, 572–580.
- Fenicia, F., D. Kavetski, and H. H. G. Savenije (2011), Elements of a flexible approach for conceptual hydrological modeling. 1: Motivation and theoretical development, *Water Resour. Res.*, *47*, W11510, doi:10.1029/2010WR010174.
- Heerwaarden, C. C., J. V. Arellano, A. F. Moene, and A. A. M. Holtslag (2009), Interactions between dry-air entrainment, surface evaporation and convective boundary-layer development, *Q. J. R. Meteorol. Soc.*, *135*, 1277–1291.
- Hobbins, M. T., J. A. Ramirez, T. C. Brown, and L. H. J. M. Claessens (2001a), The complementary relationship in estimation of regional evapotranspiration: The complementary relationship areal evapotranspiration and advection-aridity models, *Water Resour. Res.*, *37*(5), 1367–1387.
- Hobbins, M. T., J. A. Ramirez, and T. C. Brown (2001b), The complementary relationship of regional evapotranspiration: An enhanced Advection-Aridity model, *Water Resour. Res.*, *37*(5), 1389–1403.
- Huntington, J., J. Szilagyi, S. Tyler, and G. Pohl (2011), Evaluating the Complementary Relationship for estimating evapotranspiration from arid shrublands, *Water Resour. Res.*, *47*, W05533, doi:10.1029/2010WR009874.
- Kahler, D. M., and W. Brutsaert (2006), Complementary relationship between daily evaporation in the environment and pan evaporation, *Water Resour. Res.*, *42*, W05413, doi:10.1029/2005WR004541.
- Koster, R. D., and M. J. Suarez (1996), Energy and water balance calculations in the Mosaic LSM, *NASA Tech. Memo. NASA TM-104606*, vol. 9, 60 pp., Goddard Space Flight Cent., Greenbelt, Md.
- Kustu, M. D., Y. Fan, and M. Rodell (2011), Possible link between irrigation in the U.S. High Plains and increased summer streamflow in the Midwest, *Water Resour. Res.*, *47*, W03522, doi:10.1029/2010WR010046.
- Lhomme, J. P. (1997), A theoretical basis for the Priestley-Taylor coefficient, *Boundary Layer Meteorol.*, *82*, 179–191.
- Liang, X., D. P. Lettenmaier, E. F. Wood, and S. J. Burges (1994), A simple hydrologically based model of land surface water and energy fluxes for GCMs, *J. Geophys. Res.*, *99*(D7), 14,415–14,428.
- McMahon, T. A., M. C. Peel, L. Lowe, R. Srikanthan, and T. R. McVicar (2013a), Estimating actual, potential, reference crop and pan evaporation using standard meteorological data: A pragmatic synthesis, *Hydrol. Earth Syst. Sci.*, *17*, 1331–1363, doi:10.5194/hess-17-1331-2013.
- McMahon, T. A., M. C. Peel, and J. Szilagyi (2013b), Comment on the application of the Szilagyi–Jozsa advection–aridity model for estimating actual terrestrial evapotranspiration in “Estimating actual, potential, reference crop and pan evaporation using standard meteorological data: A pragmatic synthesis” by McMahon et al. (2013), *Hydrol. Earth Syst. Sci.*, *17*, 4865–4867, doi:10.5194/hess-17-4865-2013.
- Mesinger, F., et al. (2006), North American Regional Reanalysis, *Bull. Am. Meteorol. Soc.*, *87*, 343–360.
- Monteith, J. L. (1965), Evaporation and environment, in *Symposium of the Society of Experimental Biology on The State and Movement of Water in Living Organisms*, vol. 19, edited by G. E. Fogg, pp. 205–234, Cambridge Univ. Press, Cambridge, U. K.
- Morton, F. I. (1983), Operational estimates of areal evapotranspiration and their significance to the science and practice of hydrology, *J. Hydrol.*, *66*, 1–76.

- Penman, H. L. (1948), Natural evaporation from open water, bare soil, and grass, *Proc. R. Soc. London, Ser. A*, *193*, 120–146.
- Priestley, C. H. B., and R. J. Taylor (1972), On the assessment of surface heat flux and evaporation using large-scale parameters, *Mon. Weather Rev.*, *100*(2), 81–92.
- Ramirez, J. A., M. T. Hobbins, and T. C. Brown (2005), Observational evidence of the complementary relationship in regional evaporation lends strong support for Bouchet's hypothesis, *Geophys. Res. Lett.*, *32*, L15401, doi:10.1029/2005GL023549.
- Rigby, J. R., Yin J., Albertson, J. D., and A. Porporato (2015), Approximate analytical solution to diurnal atmospheric boundary-layer growth under well-watered conditions, *Boundary Layer Meteorol.*, *156*, 73–89, doi:10.1007/s10546-015-0018-8.
- Sheffield, J., B. Livneh, and E. F. Wood (2012), Representation of terrestrial hydrology and large-scale drought of the continental United States from the North American Regional Reanalysis, *J. Hydrometeorol.*, *13*, 856–876, doi:10.1175/JHM-D-11-065.1.
- Szilagyi, J. (2007), On the inherent asymmetric nature of the complementary relationship of evaporation, *Geophys. Res. Lett.*, *34*, L02405, doi:10.1029/2006GL028708.
- Szilagyi, J. (2013), Recent updates of the Calibration-Free Evapotranspiration Mapping (CREMAP) method, in *Evapotranspiration—An Overview*, edited by S. Alexandris, INTECH, Rijeka, Croatia, ISBN: 980-953-307-541-4. [Available at <http://www.intechopen.com/books/evapotranspiration-an-overview>.]
- Szilagyi, J. (2014a), Temperature corrections in the Priestley-Taylor equation of evaporation, *J. Hydrol.*, *519*, 455–464, doi:10.1016/j.jhydrol.2014.07.040.
- Szilagyi, J. (2014b), MODIS-aided water-balance investigations in the Republican River basin, USA, *Period. Polytech. Civ. Eng.*, *58*(1), 33–46.
- Szilagyi, J., and J. Jozsa (2008), New findings about the complementary relationship-based evaporation estimation methods, *J. Hydrol.*, *354*(1–4), 171–186.
- Szilagyi, J., and J. Jozsa (2009), Analytical solution of the coupled 2-D turbulent heat and vapor transport equations and the complementary relationship of evaporation, *J. Hydrol.*, *372*, 61–67.
- Szilagyi, J., and A. Schepers (2014), Coupled heat and vapor transport: The thermostat effect of a freely evaporating land surface, *Geophys. Res. Lett.*, *41*, 435–441, doi:10.1002/2013GL058979.
- Szilagyi, J., M. Hobbins, and J. Jozsa (2009), A modified Advection-Aridity model of evapotranspiration, *J. Hydrol. Eng.*, *14*(6), 569–574, doi:10.1061/(ASCE)HE.1943-5584.0000026.
- Szilagyi, J., A. Kovacs, and J. Jozsa (2011), A calibration-free evapotranspiration mapping (CREMAP) technique, in *Evapotranspiration*, edited by L. Labedzki, INTECH, Rijeka, Croatia, ISBN: 978-953-307-251-7. [Available at <http://www.intechopen.com/books/show/title/evapotranspiration>.]
- United States Department of Agriculture (USDA) (2014), 2012 Census of Agriculture, *AC-12-A-51*, Natl. Agric. Stat. Serv., Washington D. C.
- Wang, K., and R. E. Dickinson (2012), A review of global terrestrial evapotranspiration: Observation, modeling, climatology, and climatic variability, *Rev. Geophys.*, *50*, RG2005, doi:10.1029/2011RG000373.
- Wu, R., Q. Ge, X. Zhan, F. Guan, and S. Yao (2014), Drought monitoring based on simulated surface evapotranspiration by BEPS model, *J. Nat. Disasters*, *23*(1), 7–16.